Colloid Polym Sci 280: 267–273 (2002)

ORIGINAL CONTRIBUTION

Volker Herrmann
Klaus Unseld
Hans-Bernd Fuchs

The scale behavior of fillers in elastomers by means of indentation tests

Received: 15 May 2001
Accepted: 18 August 2001

V. Herrmann (✉) · K. Unseld
H.-B. Fuchs
Dunlop GmbH, Chemical Technology
Dunlopstrasse 2, 63450 Hanau
Germany
e-mail: volker.herrmann@dunlop.de
Tel.: +49-6181-681987
Fax: +49-6181-685987

Abstract Indentation tests were carried out on a carbon black filled rubber sample on different length scales. The experiments covered the range from aggregation of particles on the submicron scale up to structures which represent the bulk properties of the sample on the millimeter scale. The local stiffness was used to visualize the areas investigated; therefore, mechanical images were obtained for all length scales. So-called "mechanical units" were defined for every scale. The size distribution curves for the mechanical units were analyzed and they were found to be non-Gaussian-shaped for every scale. Moreover, the distribution curves of the mechanical units are similar to the distribution curves of particles and aggregates obtained by electron microscopy reported in the literature. Evaluation by means of fractal analysis led to fractal dimensions for the mechanical units. It could be shown in the present case that the fractal dimension $D \approx 1.24$ of the mechanical units in the range of submicrons up to several hundred microns is in good agreement with that of the filler aggregates proposed in the literature. Furthermore, D is constant over a wide range of about 6 decades in area scale starting from aggregates up to the size of agglomerates. This leads to the conclusion that the local arrangement of the filler ensembles seems to be self-similar from the smallest scale of aggregation of particles up to the largest formation observed by indentation testing on the millimeter scale.

Keywords Atomic force microscopy · Dynamic indentation · Mechanical imaging · Fractal dimension · Carbon black morphology

Introduction

In the first half of the last century carbon black incorporated in rubber, initially to cheapen the product, was found to be a suitable ingredient for reinforcement. In the following years much effort was done in the enlightenment of the mechanism of the reinforcement and the role of the microstructure of the filler [1]. Later, relations between the dispersion of carbon black and the physical properties of the rubbers were found by the help of microscopy [2–4]. In recent years a rising popular method to characterize the type of filler is the fractal analysis of filler aggregates by means of microscopy. In the literature it is reported that the fractal dimension, D, of the filler aggregates varies for the different grades of carbon black [5–7] and is an indicator for the reinforcement potential of the filler. D of the filler aggregate was found to correlate with mechanical properties of themacroscopic system, for example, the modulus [5]. The question about the link between the microscopic and the macroscopic system arises. In this work indentation methods were performed for the characterization of "mechanical units" resulting from carbon black ensembles from the micro to the macro system.

Morphology of carbon black

Carbon black [1, 8] used in the rubber industry for reinforcement consists of essentially spherical colloidal particles made up of quasi-graphitic crystallites [1]. High-resolution scanning tunneling microscopy images reveal the ordered structure of the carbon crystallites [9–11]. The size of the particles ranges from about 100 Å to a few thousand angstroms [5, 10, 12]. The smaller the particle the higher the reinforcing potential of the filler [13]. These particles exist in various forms of aggregation, the extent of this aggregation is referred to as "structure". Typical length scales for the aggregates are 50–500 nm [5, 10, 13–17]. Depending on the mixing process, the aggregates are able to cluster together to form so-called agglomerates, which have length scales from 10 to 10^3 μm [18]. Early experiments by Payne [19] led to the existence of filler–filler linkages and there is evidence that carbon black is also able to form an agglomeration network which can penetrate the whole body of a rubber sample [20, 21]. At certain loadings a percolating network structure is to be expected [22] and can be verified experimentally [23].

Fractal analysis

The characteristic feature of fractal objects is the high complexity and randomness of their pattern. It is impossible to classify them by terms of classical Euclidean geometry with integer dimensions. In a Euclidean space the dimension of a line is $D = 1$ and that of a surface is $D = 2$. Any complex object between these two, for example, a very irregular and broken curve, can be described best by a dimension between 1 and 2, a so-called "fractal dimension" [24] ("fractus" means "broken" in Latin). Mandelbrot [25] used this idea 1967 to investigate the complexity of coastlines and boundaries of different countries. Whereas mathematical fractals such as the Koch curve or the Sierpinski curve are regular and exactly self-similar at every length scale [24], fractal patterns found in nature are usually random [26]; therefore, the self-similarity of random fractals is statistical and usually exists only over a finite range of length scales [26]. In the present study the perimeter–area relation due to Mandelbrot was used to investigate the boundaries of structures as defined in a following section on different length scales. The relation used is shown in the following equation [24]:

$$L(\delta) = C\delta^{(1-D)}A(\delta)^{D/2} \quad , \tag{1}$$

where L is the perimeter of the structure, A is the area of the structure, δ is a yardstick length, C is a constant, and D is the fractal dimension.

For $\delta \to 0$, $L \to \infty$ and A remains finite. Since for a self-similar object D is independent of δ, the only condition for Eq. (1) to hold is a δ small enough to measure the smallest feature of the structures. If this condition is fulfilled, the slope of a plot $\log L$ versus $\log A$ gives the fractal dimension of a coastline profile of the structures within a self-similar range of a random fractal.

Experimental

Sample preparation

The sample investigated here was a sulfur cross-linked carbon black filled vulcanisate (for the formulation, see Table 1). The compound was mixed in a laboratory Brabender Banbury mixer and afterwards passed through a laboratory mill and sheeted out. The mixing process ensures maximum filler dispersion according to a prior investigation [27] (see also Table 1). The sample was vulcanized to a thickness of 2 mm in a heating press at 160 °C to maximum cross-linking using a Monsanto MDR2000 E. The surface of the sample was then investigated by indentation methods as follows.

Indentation methods

The indentation methods used in this investigation were atomic force microscopy (AFM) [28] and a recently introduced new method, in the following called the dynamic indentation method (DIM) [29–33]. Both methods work by the same principle but on different length scales. In every case the surface of the sample was examined with a sharp tip in contact with the sample. The DIM works with a conical tip with a semivertical angle of 14° and a tip radius of 1 μm. For the realized AFM indentations the tip can be regarded as a cone with a semivertical angle of around 10–20° and a tip radius of 20 nm. Defined indentations can be carried out and a quantity proportional to the force, or in the case of the DIM directly the resulting force, can be detected. The local mechanical information (local stiffness) is obtained by the ratio of force and corresponding indentation. In both cases there is a possibility to scan a defined area of the sample and to get mechanical images, so-called "stiffness images".

The AFM was used in two different scan modes: The pulsed force mode (WITec) [34] and the layered imaging mode (Topometrix) in a way described elsewhere [35], in the following called AFM_{PFM} and AFM_{LIM}, respectively. The indentation depths were in the range of a few hundred nanometers, dependent on the stiffness of the local spots. In the case of the AFM_{PFM} the scan range was 3 μm × 3 μm and in the case of the AFM_{LIM} the scan range was 50 μm × 50 μm.

Table 1 Compound formulation (phr) and mixing procedure

Formulation	
E-SBR 1500	100
Zinc oxide	3
Stearic acid	2
N220	50
TBBS	1
Sulfur	1
Mixing procedure	
0 min	Polymer
2 min	Zinc oxide/stearic acid/N220
14 min	TBBS/sulfur
18 min	Dump

The DIM was used in the dynamic mode in two ways:

1. Constant force mode (DIM_{CFM}). Here the tip penetrates the surface until a force of 2 mN is reached. The indentation depth in the present case was then of about 10 μm. After that a sinusoidal oscillation of the tip of ± 3 μm and a frequency of 15 Hz was carried out.
2. Constant depth mode (DIM_{CDM}). The tip penetrates the surface with an indentation depth of 50 μm, followed by an oscillation of ± 5 μm with a frequency of 10 Hz.

The DIM investigation corresponds to an area in the x-and y directions of 4×4 mm in both cases. All the measurements were performed at room temperature. The mechanical images were created with SigmaPlot 2000 V.6.00 (SPSS) in a black–white contrast, where the black spots mean high stiffness values. In the following the black (''hard'') spots are called ''mechanical units''. Here it should be pointed out that the sizes of the structures in the mechanical images generally depend on the agreement as to what is to be regarded as ''hard''. The common procedure followed in this study was to entitle every stiffness value, x, as ''hard'' which deviated more than the standard deviation, σ, from the average value, $\bar{x}$, of the whole image, that means $x_{\text{''hard''}} > \bar{x} + \sigma$. Whereas the sizes of the structures depend slightly on this agreement, the fractal dimension and the shape of the size distribution were assumed to be independent. Enough images were created for every length scale to allow at least 500 mechanical units to be evaluated for the size distribution curves. The respective yardsticks to measure the structures were the ratio of the edge of the image to the number of pixels in the same direction. This condition always ensures a yardstick small enough with respect to the smallest cluster according to Kaye [36]. The perimeters and the areas of the black spots according to the previous section were determined by an image analysis program (SigmaScan Pro V.5.0.0, SPSS).

Results and discussion

Typical mechanical images of the AFM and DIM_{CFM} investigations are shown in Fig. 1. The mechanical units as defined in the previous section are depicted in black. The lengths of the respective image edges are shown in the figure. The number of pixels for every image is 200×200. For every structure the diameter for the equivalent circle is calculated. The relative frequencies of these diameters are shown in Fig. 2. Despite the fact that the curves show the distribution of local mechanical behavior on different length scales, a certain relationship of these shapes to the aggregate size distributions obtained by other methods [5, 10, 13, 14, 15, 16, 17] can be recognized. It seems reasonable that the mechanical units more or less result from carbon black entities. It was shown that the pulsed force mode accounts for carbon black particles or aggregates by higher stiffness values than the rubber matrix [34, 37, 38]. In the AFM_{PFM} investigation shown at the top of Fig. 2, the first peak can be detected at 20 nm, which coincides with the diameter of the primary particle of N220 [5, 39]. Further peaks due to aggregation of particles can be detected. A bimodal distribution due to primary particles and their aggregation was obtained in AFM investigation by Trifonova-van Haeringen et al. [40]. Therefore, the particles seem to create clusters with

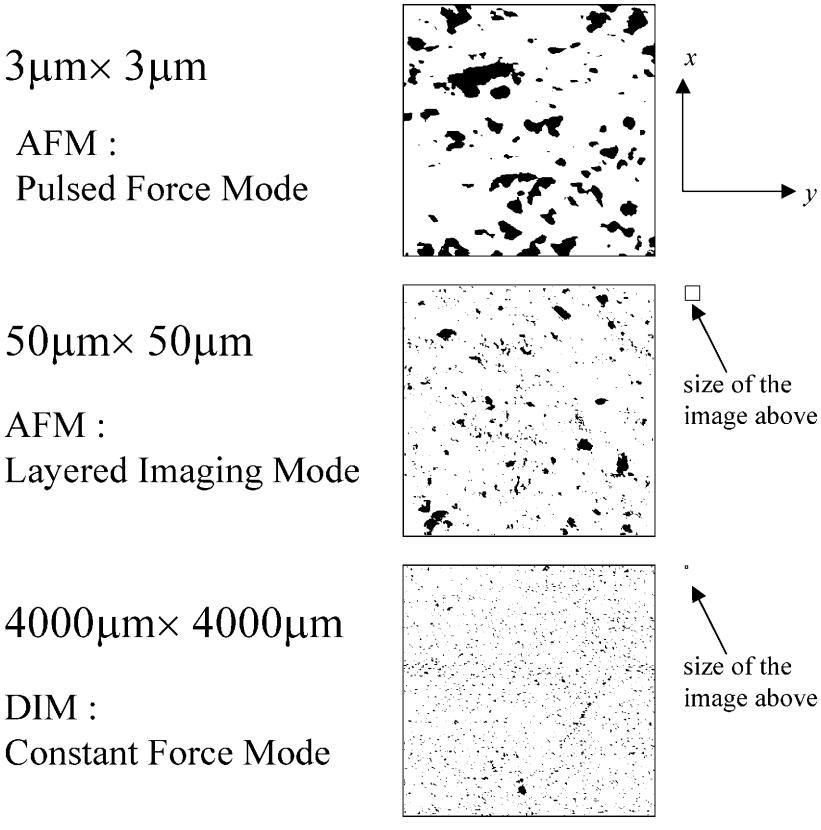

Fig. 1 Mechanical stiffness images of a carbon black filled rubber sample on different length scales. The number of pixels is 200×200 for every image. The stiffnesses of the black spots are higher than the average value plus standard deviation of the whole image

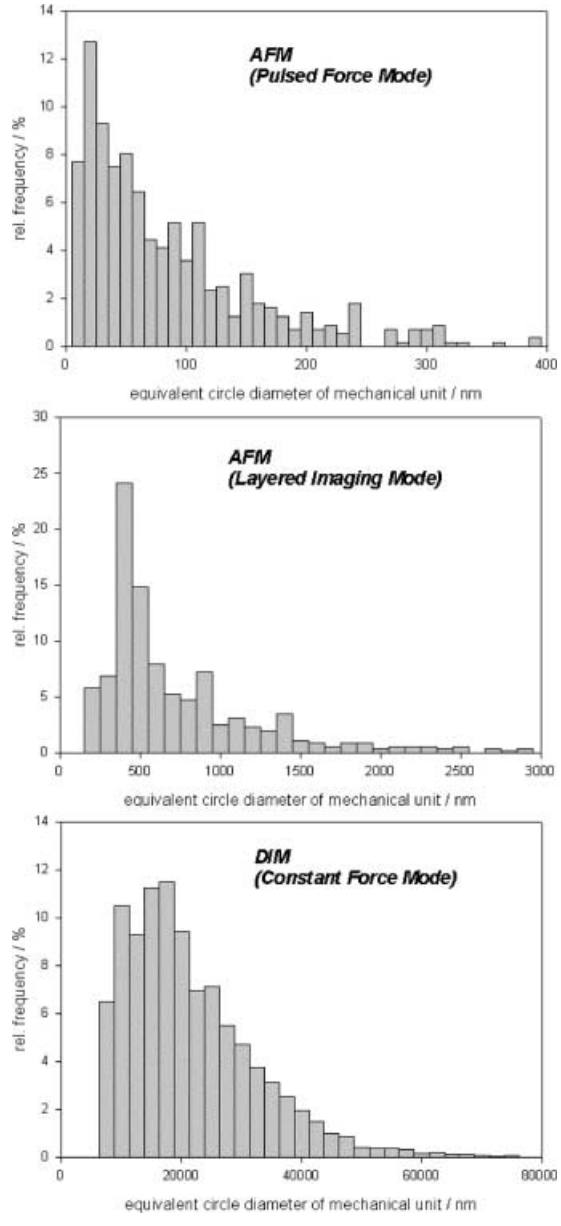

Fig. 2 Distribution curves of the equivalent circle diameters of the black structures in Fig. 1 for every length scale. Each distribution represents at least 500 structures

different sizes of several hundred nanometers. For the AFM_{LIM} investigation, Fig. 2, center, the most frequent diameter can be detected at 400 nm. Since the indentation depth here is higher than in the AFM_{PFM}, this method seems to be related to the stiffness of the cooperating ensembles on the length scale described later. The local stiffness then is a result of the size and/or frequency of the clusters on this scale. Regarding the DIM_{CFM} investigation, Fig. 2, lower graph, a further length scale is observed. The dynamic indentation depth of the DIM_{CFM} was $\pm 3\ \mu$m; hence, this method is supposed to be sensitive for the structures displayed in the middle of Fig. 2 by the AFM_{LIM}. Therefore, the DIM images account for the carbon black density distribution on the micron scale [31–33]. The use of the conical tips in all the investigations ensures high locality of the mechanical information and therefore the visualization of the structures. Thus, according to Sneddon [41] the radius, a, of contact between tip and sample by the use of a cone can be estimated by

$$a = \frac{2}{\pi} h \tan \alpha \ , \tag{2}$$

where h is the indentation depth and α is the semivertical (inner) angle of the tip; therefore, the contact radius for the DIM is 16%, for AFM 11–23% of the indentation depth, and the information is locally limited. For the DIM and the AFM_{LIM} investigation the distance between neighboring points was chosen to avoid overlaps with the area of the indentation done before. For the AFM_{PFM} investigation the step size was smaller than the expected contact area; however, the pulsed force mode has already proven to be noninvasive for the imaging of carbon black particles and aggregates owing to the gentle procedure of this mode [34, 37, 38]. The evaluation of the perimeters and areas of the black spots in the mechanical images lead to the $\log L$ versus $\log A$ plot shown in Fig. 3. One obtains linear behavior for every s scale, where the slope of each curve immediately delivers the fractal dimension, D. As can be seen again, the structures detected by AFM start at about 10 nm up to several microns. The fractal dimensions obtained and the respective correlation coefficients, r, are depicted in the figure. The fractal dimension for the AFM_{PFM} investigation is $D_{AFMPFM} = 1.119$, the same for the AFM_{LIM} is $D_{AFMLIM} = 1.245$. The structures observed by the DIM start at several microns up to about 100 μm. In this case the fractal dimension obtained is $D_{DIMCFM} = 1.235$ for the constant force mode and $D_{DIMCDM} = 1.241$ for the constant depth mode. Gerspacher and coworkers [6, 7] found the fractal dimension of the aggregate boundary for N220 to be $D = 1.279$ with an interval of 95% confidence of $D = 1.24$–1.32 by transmission electron microscopy (TEM) micrographs. As also shown in the literature, D varies for different aggregate shapes [5]. So, for N220, D was found to be 1.15 for ellipsoidal aggregate shapes, 1.29 for linear shapes and 1.32 for branched shapes of aggregates even within one grade of carbon black; therefore, the fractal dimensions obtained by AFM_{LIM} and DIM are in good relationship to the fractal dimensions reported for the N220 aggregates in the literature. However, the statistical self-similarity seems to be limited to the scale of the particles of carbon black. It was postulated and shown for a simulated aggregate by Kaye [42] that a discontinuity is supposed in the plot owing to changing fractal dimension when reaching the subunits forming the

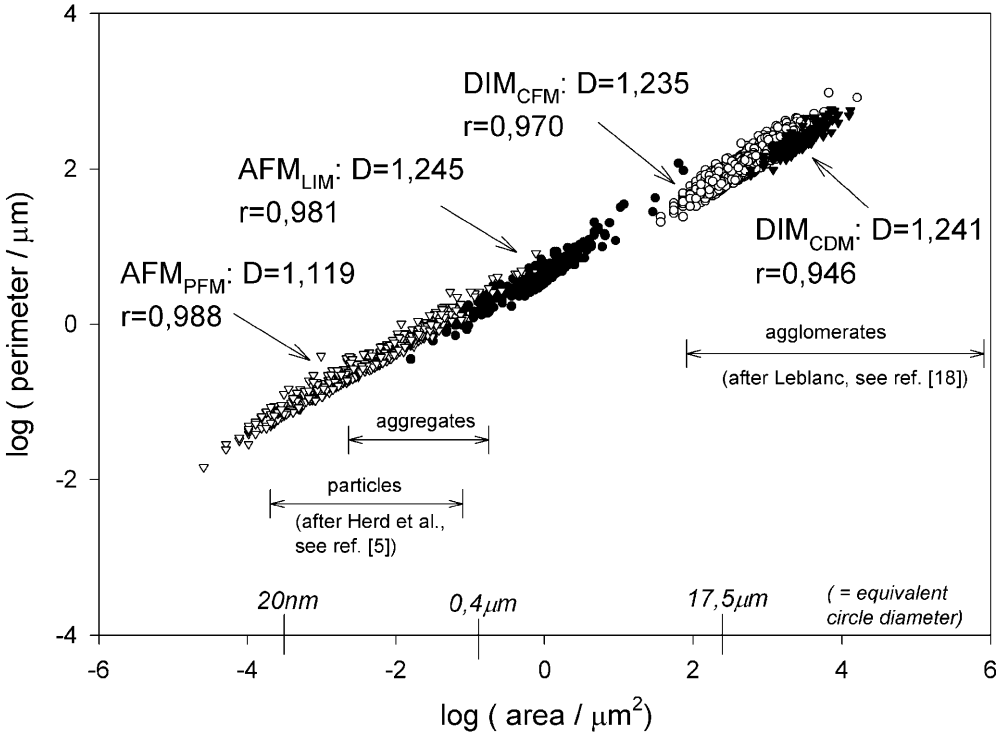

Fig. 3 Log$L$ versus log$A$ plot of the structures displayed in Fig. 1. The fractal dimensions for the respective methods obtained are indicated in the figure. The position of the carbon black entities according to the literature and the respective maxima of Fig. 2 are displayed

aggregate. This was verified by Flook [43] for the profile of a real carbon black aggregate. A change in the fractal dimension at the transition from particle to aggregate from $D = 1.07$ to $D = 1.37$ was found. This obviously represents the lower limit of self-similarity of the carbon black structures, and this seems to emerge by the smaller fractal dimension at the lowest scale $D_{\mathrm{AFMPFM}} = 1.119$, which is significantly smaller within the limit of error than D for $\mathrm{AFM_{LIM}}$ or for DIM. Taking into account that the fractal dimension here was determined by indentation tests where the stiffness of the surface is the requested property, the results are in good agreement with the results in the literature. Overall, we have to keep in mind that the structures evaluated are "mechanical units" obtained by indentation tests. It is suggested in every case that the respective carbon black entities result in higher local stiffness. Slight deviations of this idea might result from the influence of cross-link density fluctuation on the local stiffness [34, 44]. Moreover, by the validity over the range of 6 decades in area scale, starting from aggregates up to structures of length of around 100 μm, the interesting question about the organization of the carbon black structures arises. The formation of the mechanical units shows self-similarity in the sense of Mandelbrot's definition [25]. Assuming the fact that the local stiffness represents the carbon black structures on every length scale, the clustering of carbon black seems to obey the same principle from primary particle to aggregates as well as from aggregates to agglomerates. Concerning this, interesting models have been developed recently [45]. A further attempt to describe the aggregation process by diffusion-limited clustering was done by Kolb [46]. In his model reversible aggregation and fragmentation occur independently from each other with different time constants. In the steady state the equilibrium cluster size is given. It could be shown that the cluster size distribution has a scaling form and shows non-Gaussian behavior with a shift on the right-hand scale with respect to higher numbers of large clusters. By varying the diffusing velocity of a cluster, the fractal dimension of the system can be modified. According to Kolb the cluster size distribution should show the same shape for different length scales. The size distributions for different entities of carbon black are shown in Fig. 4. The upper figure shows the distribution for carbon black particles of N115 by TEM [12]; the lower figure displays the same for carbon black aggregates of N220 also investigated by electron microscopy [14]. Since the electron microscopy displays the formation of the carbon black particles and aggregates, the indentation tests performed in this study illustrate the mechanical effect of these ensembles. Therefore, the fact that even for the mechanical units similar shapes of distribution curves are obtained gives a further hint that the indentation tests performed in this study account for the reinforcing properties of the filler. Furthermore, Kolb's model regarding the diffusion-limited cluster

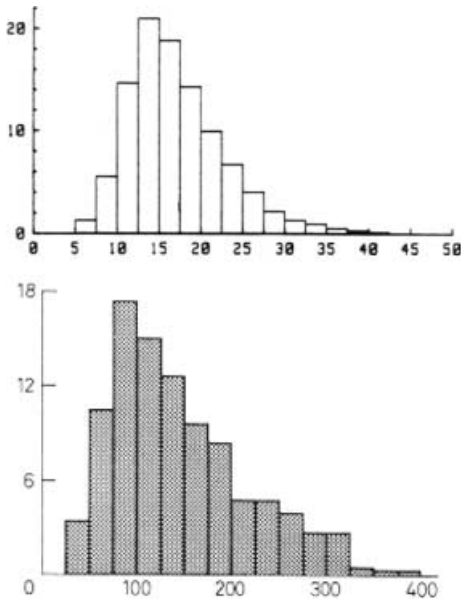

Fig. 4 Distribution curves of carbon black entities by electron microscopy according to the literature. *Top*: Primary particle of N115 [12]; *bottom*: aggregates of N220 [14]. The *x*-axis displays the particle diameter or the length of the aggregates in nanometers; the *y*-axis displays the relative frequency

aggregation process seems to describe the principles of carbon black clustering.

Conclusion

The indentation tests used in this study have proven to be a useful tool to investigate the morphology of carbon black loaded rubbers on different length scales. The fractal dimension, D, of the local stiffness is in good agreement with that obtained by TEM of the carbon black aggregates reported in the literature. Furthermore, D seems to be constant over a range of 6 decades in area scale. This was never described for such a large interval in the literature before. The validity of this observation extends to the millimeter scale, where bulk properties are represented. Because of the direct relation of stiffness and modulus [30–32], indentation tests are suitable for the investigation of the relationship between carbon black morphology and macroscopic mechanical behavior of a rubber sample. In the future it might be a matter of interest to investigate different grades of fillers or to study the influence of mixing conditions of carbon black on the fractal dimension on different length scales and its relation to macroscopic mechanical data, such as modulus, tensile strength, or abrasion resistance. A further interesting study could be the fractal dimension under strain on the scales investigated in this work.

Acknowledgements The authors gratefully acknowledge the contributions of B. Blümich. Many thank to H. Schnecko for constructive advice. Furthermore, the authors wish to thank H.-G. Kilian for stimulating discussions.

References

1. Kraus G (1965) Reinforcement of elastomers. Wiley, New York
2. Sweitzer CW, Hess WM, Callan JE (1958) Rubber World 138:869
3. Sweitzer CW, Hess WM, Callan JE (1958) Rubber World 139:74
4. Boonstra BB, Medalia AI (1963) Rubber Chem Technol 36:115
5. Herd CR, McDonald GC, Hess WM (1992) Rubber Chem Technol 65:107
6. Gerspacher M, O'Farrell CP (1991) Elastomerics 123:35
7. Gerspacher M, O'Farrell CP (1992) Kautsch Gummi Kunstst 45:97
8. Donnet J-B, Voet A (1976) Carbon black. Dekker, New York
9. Donnet J-B, Custodero E (1992) Carbon 30:813
10. Hess WM, Herd CR, Sebok EB (1994) Kautsch Gummi Kunstst 47:328
11. Göritz D, Raab H, Fröhlich J, Maier PG (1999) Rubber Chem Technol 72:929
12. Wolff S (1987) Thesis. Universite de Haute Alsace
13. Patel AC, Lee K (1990) Elastomerics 122:14
14. Hess WM, Chirico VE, Burgess KA (1973) Kautsch Gummi Kunstst 26:344
15. Hess WM, McDonald GC, Urban E (1973) Rubber Chem Technol 46:204
16. Alshuth T, Schuster RH, Kämmer S (1994) Kautsch Gummi Kunstst 47:702
17. Maas S, Gronski W (1994) Kautsch Gummi Kunstst 45:409
18. Leblanc JL (1995) Plast Rubber Compos Process Appl 24:241
19. Payne AR (1961) Rubber Plast Age 42:963
20. Kraus G (1984) J Appl Polym Symp 39:75
21. Wang M-J, Wolff S, Tan E-H (1993) Rubber Chem Technol 66:178
22. Klüppel M (1997) Kautsch Gummi Kunstst 50:282
23. O'Farrell CP, Gerspacher M, Nikiel L (2000) Kautsch Gummi Kunstst 53:701
24. Feder J. (1988) Fractals. Plenum, New York, p 201
25. Mandelbrot BB (1967) Science 156:636
26. Reynolds PJ (1993) On clusters and clustering. Elsevier, Amsterdam
27. Bode M (1995) Diploma thesis. FH Frankfurt/Dunlop GmbH
28. Binnig G, Quate CF, Gerber C (1986) Phys Rev Lett 56:930
29. Unseld K, Albohr O, Herrmann V, Fuchs H-B (2000) Kautsch Gummi Kunstst 53:52
30. Unseld K, Herrmann V, Fuchs H-B (2000) Kautsch Gummi Kunstst 53:518
31. Unseld K, Herrmann V, Klug A, Fuchs H-B (2000) Kautsch Gummi Kunstst 53:644
32. Unseld K, Herrmann V, Fuchs H-B (2001) Kautsch Gummi Kunstst 54:397
33. Herrmann V, Unseld K, Fuchs H-B Kautsch Gummi Kunstst (in press)
34. Rosa A, Hild S, Marti O (1996) Polym Prepr Am Chem Soc Div Polym Chem 37:616
35. Herrmann V, Unseld K, Fuchs H-B (2001) Kautsch Gummi Kunstst 54:453
36. Kaye BH (1989) In: Avnir D (ed) The fractal approach to heterogeneous chemistry. Wiley, New York, p 62
37. Rosa-Zeiser A (1997) Thesis. Universität Ulm

38. Rosa-Zeiser A, Weilandt E, Hild S, Marti O (1997) Meas Sci Technol 8:1333
39. Zerda TW, Yang H, Gerspacher M (1992) Rubber Chem Technol 65:130
40. Trifonova-van Haeringen D, Schönherr H, Vancso GJ, van der DoesL, Noordermeer JWM, Janssen PJP (1999) Rubber Chem Technol 72:862
41. Sneddon IN (1965) Int J Eng Sci 3:47
42. Kaye BH (1978) Powder Technol 21:1
43. Flook AG (1978) Powder Technol 21:295
44. Engelbert van Bevervoorde-Meilof WW, Trifonova-van Haeringen D, Vancso GJ, van der Does L, Bantjes A, Noordermeer JWM (2000) Kautsch Gummi Kunstst 53:426
45. Kilian HG, Metzler R, Zink B (1997) J Chem Phys 107:8697
46. Kolb M (1986) J Phys A Math Gen 19:L263